Regenerative Therapy 29 (2025) 292–302

Contents lists available at ScienceDirect

Regenerative Therapy

journal homepage: http://www.elsevier.com/locate/reth

Original Article

In vivo evaluation of biocompatibility and biodegradation of porcine collagen membranes

Seon Ae Kim [a], Eun Jeong Go [a], Bo Seung Bae [a, d], Jae Woong Jung [a], Mi-La Cho [b], Asode Ananthram Shetty [c], Seok Jung Kim [a, *]

[a] Department of Orthopedic Surgery, College of Medicine, The Catholic University of Korea, Seoul, Republic of Korea
[b] Department of Pathology, College of Medicine, The Catholic University of Korea, Seoul 06591, Republic of Korea
[c] Institute of Medical Sciences, Faculty of Health and Social Care, Canterbury Christ Church University, United Kingdom
[d] Department of Medicine, Graduate School, Kyung Hee University, 26, Kyungheedae-ro, Dongdaemun-gu, 02453 Seoul, Republic of Korea

ARTICLE INFO

Article history:
Received 20 December 2024
Received in revised form
18 February 2025
Accepted 19 March 2025

Keywords:
Collagen membrane
Biocompatibility
Inflammation
Atelocollagen

ABSTRACT

Introduction: Collagen-based materials differ in absorption time, biodegradation patterns, and inflammatory cell infiltration. This study aimed to evaluate the biocompatibility and biodegradation of native, differently processed, and cross-linked porcine collagen membranes implanted in the subcutaneous tissue of rats, following ISO 10993-6:2016.

Methods: Sixty Sprague–Dawley rats were randomly divided into four groups: Group 1 (lyophilized 3 % porcine type I collagen membrane), Group 2 (lyophilized 3 % porcine type I collagen membrane, dehydrothermal [DHT]), Group 3 (1,4-butanediol diglycidyl ether [BDDE] cross-linked, lyophilized 3 % porcine type I collagen), and Group 4 (BDDE cross-linked, lyophilized 3 % porcine type I collagen, DHT). The experimental periods were 1, 2, 4, 8, and 12 weeks, with three animals per group per period. After each period, specimens were extracted and analyzed for membrane structure, biodegradation, cell infiltration, angiogenesis, tissue integration, and foreign body reaction using histological staining and scoring according to ISO 10993-6:2016.

Results: The cross-linked collagen membrane groups maintained their porous structure, with cell infiltration and blood vessel formation observed within this structure. Non-cross-linked collagen membranes (Group 1) appeared as lumps under the subcutaneous tissue and exhibited minimal or no response throughout the observation periods. Groups 2 and 4 biodegraded the fastest. Group 2 membranes were not detected in the subcutaneous tissue at 8 weeks, classified as a slight response. Cross-linked collagen membranes in all groups showed a slight response, whereas Group 4 exhibited a moderate response (11.0–16.9) only at 12 weeks. The tissue response to collagen membranes in all groups aligned with physiological inflammatory processes, scoring from minimal or no response (0.0–5.9) to slight response (6.0–10.9), confirming their biocompatibility.

Conclusions: Cross-linking methods, temperature, and chemical reagents influence collagen membrane properties. Cross-linked collagen formed a porous structure, and high-temperature DHT cross-linking accelerated the biodegradation of the collagen membrane.

Abbreviations: BDDE, 1,4-Butanediol diglycidyl ether; DAB, 3,3′-Diaminobenzidine; DHT, Dehydrothermal treatment; ECM, Extracellular matrix; HE, Hematoxylin and eosin; ISO, International Organization for Standardization; PLA, Polylactic acid; PLGA, Polylactic-co-glycolic acid; PGA, Polyglycolic acid; PMN, Polymorphonuclear cells.

* Corresponding author. Department of Orthopedic Surgery, Uijeongbu St. Mary's Hospital, College of Medicine, The Catholic University of Korea, 271, Cheonbo-ro, Uijeongbu-si, Gyeonggi-do, Republic of Korea.
E-mail address: peter@catholic.ac.kr (S.J. Kim).

Peer review under responsibility of the Japanese Society for Regenerative Medicine.

https://doi.org/10.1016/j.reth.2025.03.015

1. Introduction

The development of improved biomaterials is crucial in tissue engineering. These biomaterials must exhibit good biocompatibility, avoid side effects, and serve as excellent scaffolds for cell growth and metabolism. Additionally, biodegradability and bioabsorbability must be controlled for clinical applications. Furthermore, biomaterials require mechanical properties that withstand various stresses, a good surface conducive to cell adhesion, and malleability. Collagen accounts for approximately 30 % of the proteins present in vertebrates and is the most abundant extracellular matrix (ECM) protein [1,2]. It possesses excellent biological properties, including biocompatibility [3], tissue affinity, and the promotion of cell adhesion [4,5], migration, spreading, and proliferation. It also provides an optimal environment for cellular responses and components [6,7]. Collagen is biodegradable [5,8,9], has low antigenicity [10,11], is non-cytotoxic and anti-inflammatory [12,13], is easy to process, has abundant sources, and exhibits hydrophilic properties. Consequently, collagen is widely used in tissue engineering applications [14–17], including local drug delivery [18,19], bone augmentation around dental implants [20,21], tendon/ligament augmentation after sports injuries [22–24], spinal dura repair to prevent cerebrospinal fluid leakage [25,26], burn and wound dressing [27], and hemostasis [28,29]. However, natural collagen has low mechanical strength and a rapid decomposition rate *in vivo*, which limits its clinical applicability [30]. To overcome these limitations, synthetic polymers (lactic acid) (PLA), poly (glycolic acid) (PGA), and poly (lactic-co-glycolic acid) (PLGA) are being developed. Additionally, several cross-linking techniques [31–33], including ultraviolet light, glutaraldehyde, diphenylphosphorylazide, and hexmethylenediisocyanate, have been used to prolong biodegradation. In animal models, these methods reduce the decomposition rates compared to natural biomaterials [34–36], but they also inhibit cell adhesion and proliferation [37,38] and reduce tissue integrity and vascular distribution [18,39].

Thus, characterizing and comparing the physical, mechanical, and biological properties of collagen is essential to selecting collagen materials. Preclinical research models are valuable for assessing the safety and tissue compatibility of materials and predicting their immunogenicity in the human body. These assessments are crucial for achieving clinical applications. Therefore, this study aimed to evaluate the biocompatibility and biodegradability of various collagen membranes according to ISO 10993-6:2016 standards. Our results provide baseline data on collagen membranes under different cross-linking conditions.

2. Methods

2.1. Animals

Thirty male Sprague–Dawley rats, approximately 8 weeks old and weighing 200–250 g, were used in this study. Animal management, selection, and surgical procedures were approved by the Institutional Animal Care and Use Committee of The Catholic University of Korea, Uijeongbu St. Mary's Hospital, and were conducted in accordance with the Institute of Laboratory Animal Resources Guide for the Care and Use of Laboratory Animals (approval number: UJA2021-09A). The animals were randomly selected by an investigator and acclimatized before the experiment.

2.2. Collagen membrane preparation

Collagen membrane were prepared using collagen gel (Ubiosis, Seongam, Korea) derived from porcine dermis. Four types of collagen membranes were used: (1) lyophilized 3 % porcine type I collagen membrane; (2) lyophilized 3 % porcine type I collagen membrane, DHT; (3) 1,4-butanediol diglycidyl ether (BDDE) cross-linked, lyophilized 3 % porcine type I collagen as BDDE-crosslinked collagen; (4) BDDE cross-linked, lyophilized 3 % porcine type I collagen, DHT as BDDE-crosslinked collagen, DHT. All collagen membranes were manufactured and packaged at a size of 90 × 90 mm and were cut into 10 × 10 mm pieces for implantation.

2.3. Experimental groups

In this study, animals were divided into four groups: Group 1 (lyophilized 3 % porcine type I collagen membrane); Group 2 (lyophilized 3 % porcine type I collagen membrane, DHT); Group 3 (BDDE-crosslinked collagen); Group 4 (BDDE-Crosslinked collagen, DHT) (each group, n = 15). The groups were subdivided according to the experimental period (1, 2, 4, 8, and 12 weeks), with three animals in each group/experimental period.

2.4. Anesthesia and surgical procedures

Rats were anesthetized using 2 % isoflurane (Hana Pharm Co., Ltd. Seoul, Korea). To prepare the surgical sites, the fur on the dorsal region was shaved, and the skin was cleaned with povidone. Two 10-mm incisions were made on the right and left sides of the dorsal region (three animals per group). The skin and fascia were then separated using blunt scissors. A collagen membrane of the same size (10 mm) was implanted into the space between the skin and fascia. The incisions were sutured using nylon (Ethicon®, Johnson and Johnson, Ethicon, Cincinnati, OH, USA), and the sutured area was cleaned with gauze soaked in povidone. The same procedures (incision, displacement, and suturing) were performed for the animals in the sham group; however, no collagen membranes were implanted (Fig. 1).

2.5. Obtaining samples

After 1, 2, 4, 8, and 12 weeks, tissues were collected from three animals in each group. Samples were taken from the membrane implantation sites and the surrounding tissues, with a safety margin of approximately 5 mm on each side. All samples were fixed in 10 % buffered formalin (Sigma–Aldrich, SL, USA) for at least 24 h.

2.6. Histological analysis

After fixation, the samples were histologically processed. Briefly, the samples were embedded in paraffin, cut into 5 μm thick sections, and stained with hematoxylin and eosin (HE) for light microscopy assessment. Inflammation and macrophage expression were evaluated by immunohistochemistry. Anti-CCR7 (M1 macrophage marker; Abcam, Cambridge, MA, USA), anti-CD206 (M2 macrophage marker; Abcam), anti-CD20 (B lymphocyte marker; Abcam), and anti-CD3 (T lymphocyte marker; Abcam) antibodies were used to assess inflammatory cell infiltration into the implanted collagen membranes. Samples were deparaffinized, rehydrated in graded alcohols, and blocked with 3 % hydrogen peroxide to inhibit endogenous peroxidase activity. Epitope retrieval was performed at room temperature for 25 min using collagenase (Thermo Fisher Scientific, Waltham, MA, USA). The samples were then incubated with primary antibodies for 1 h at room temperature, and immunoreactive signals were visualized using a peroxidase-based kit (Dako, Agilent, Santa Clara, CA, USA), with 3,3′-diaminobenzidine (DAB; Dako) as the chromogen. Cell nuclei were counterstained with hematoxylin.

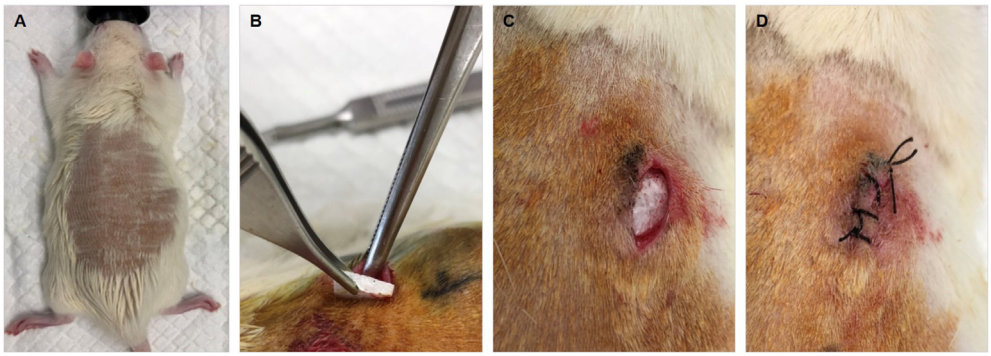

Fig. 1. Surgical procedures. (a) Shaved and cleaned dorsal region of animal. (b) Collagen membrane implantation. (c) Implanted membrane location between skin and fascia. (d) Sutured incision.

2.7. Thickness measurement

The thickness of all collagen membranes at different implantation times was measured using a programmed tool (CellSens Standard, Olympus, Japan) at 40 × microscope magnification.

2.8. Microscopic analysis

All microscopic observations and scoring were performed by three investigators. The transplanted membrane and its interface were observed, and stained tissue on the coated slide was photographed digitally using a microscope (OLYMPUS®, Tokyo, Japan). To obtain detailed image information, the cells and tissues were examined at 100 × , 200 × , and 400 × magnification and subjected to semiquantitative histological analysis. Samples from three animals were analyzed at 1, 2, 4, 8, and 12 weeks in all groups.

2.9. Evaluation of biomaterial implantation: semiquantitative histological analysis: ISO 10993-6:2016/part 6/Annex E

ISO 10993-6:2016 specifies test methods for assessing local effects after the implantation of biomaterials intended for medical devices. The total tissue response of each membrane material was scored and evaluated according to ISO 10993-6. The evaluated scores were summed and compared. Tissue response scoring and evaluation were based on (1) the number and distribution of inflammatory cells at the material–tissue interface, (2) the presence of necrosis, and (3) inflammatory responses such as neovascularization, fibrosis of the fibrous capsule, and fatty infiltration. The collagen membranes from the four groups were compared based on differences in these parameters. The total scores were categorized as non-irritant (0.0–5.9), slightly irritant (6.0–10.9), moderately irritant (11.0–16.9), or severely irritant (≥17). The measured values were presented as median, minimum, and maximum values.

2.10. Statistical analysis

All data are presented as mean ± standard deviation. Statistical analyses were performed using a two-way ANOVA with Prism (version 5.01; GraphPad Software, La Jolla, CA, US). Differences were considered statistically significant when $P < 0.05$. $^{*}P < 0.05$, $^{**}P < 0.01$, $^{***}P < 0.001$.

3. Results

3.1. Animal observations

All animals tolerated the surgical procedure well, with no necrosis or complications at the surgical site. They recovered quickly after surgery and exhibited no abnormal behavior or weight loss.

3.2. Observation of implanted membranes

Subcutaneously implanted collagen membranes were observed at weeks 1, 2, 4, 8, and 12 (Fig. 2). One week after implantation, Group 1 did not maintain its initially implanted shape (square) and showed a gel-like aggregate. The membrane in Group 2 gradually decreased in size from 1 to 4 weeks and did not remain under the subcutaneous tissue at 8 weeks. The membranes of Groups 3 and 4 maintained their shape for up to 12 weeks after implantation. None of the subcutaneously implanted collagen membranes induced local inflammation, redness, swelling, or purulence. The collagen membrane was embedded and fused well with the subcutaneous fascial tissue. The incision site and skin used for membrane implantation healed well, and the rats were healthy and active, indicating that the implanted collagen membrane had good biocompatibility.

3.3. Histopathological analysis

Subcutaneously implanted collagen membranes were collected at 1, 2, 4, 8, and 12 weeks and analyzed using HE staining.

3.4. One week post-implantation

One week after implantation, the implanted collagen membranes exhibited different structures (Fig. 3A). Group 1 failed to maintain its initial shape, which appeared as a compact lump in histological observations (Fig. 3A (a–c)). Except for Group 1, the membranes in the other groups remained intact subcutaneously and showed a multilayered porous structure. The membrane structure in Group 2 was thicker than in the other groups, which resulted in darker hematoxylin staining (blue color) (Fig. 3A (d–f)). Red blood cells were observed inside Groups 2, 3, and 4 membranes, which also showed porous structures (Fig. 3A (f,h,i,k,l), orange arrow). However, Group 1 membranes showed very few red blood cells. In all groups, the membrane was separated from the

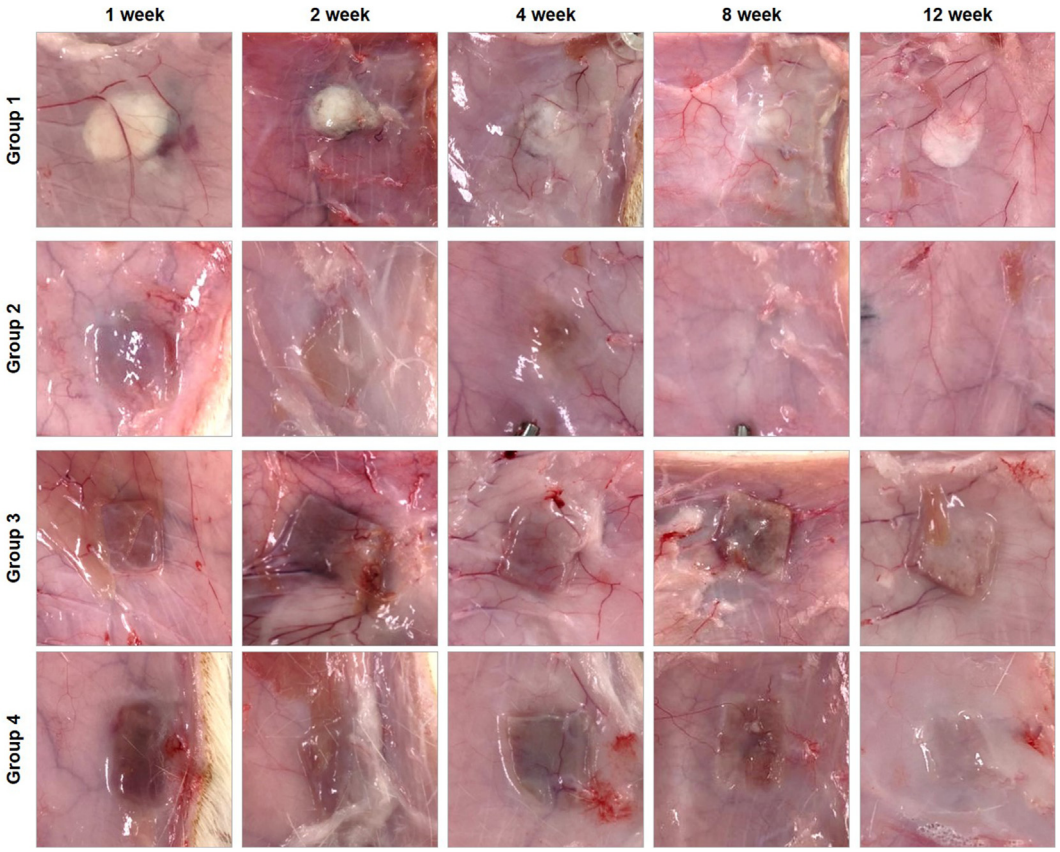

Fig. 2. Representative images of the collagen membrane at 1, 2, 4, 8, and 12 weeks after subcutaneous implantation into rats.

adjacent connective tissue (the implanted membrane region is marked with an asterisk). Fatty infiltration, tissue necrosis, and severe fibrous encapsulation were not observed in any groups.

3.5. Two weeks post-implantation

Two weeks after implantation, numerous inflammatory cells were observed in the tissue adjacent to the external surface of the implanted membrane in all groups. More inflammatory cells infiltrated the membranes compared to the 1 week after implantation (Fig. 3B) (implanted membrane region is marked with an asterisk; *). In addition, an increased macrophage infiltration was observed in all groups compared with that at 1 week. Groups 2, 3, and 4 membranes maintained a porous structure (Fig. 3B (d–l)), and increased vascularization was noted (Fig. 3B, orange arrow). Significant blood vessel formation was observed in Group 2 (Fig. 3B (e, f), orange arrow). Membranes in all the groups were surrounded by connective tissues, but no capsule formation or fibrosis was observed. Cell density decreased from the membrane surface toward the interior.

3.6. Four weeks post-implantation

Four weeks after implantation, tissue integration occurred on both sides of the membrane. Cell penetration was observed on both sides of the membrane surfaces, and the inner membrane structure was equalized after 4 weeks (the implanted membrane region is marked with an asterisk; *). In Group 1, the membrane body was reduced, and the number of cells inside and outside the membrane was lower than at 2 weeks. Small blood vessels were observed inside the membrane (Fig. 4A (c), orange arrow). In all other groups, numerous inflammatory cells were observed around the membrane, in adjacent areas, and within the inner membrane space. Additionally, many blood vessels and cells were observed.

Notably, Group 2 showed a significant decrease in the membrane body, consistent with membrane thickness measurements (Fig. 4A (d–f)). The membrane maintained its thick skeleton and porous structure. Group 3 retained the best porous structure, with thickness similar to that at initial implantation. Vascular endothelial cells inside the membrane developed into mature blood vessels, with many blood cells present (Fig. 4A (h, i), orange arrow). Group 4 maintained a porous structure, though its thickness was slightly reduced. Blood vessels and cells were observed (Fig. 4A (k, l), orange arrow).

3.7. Eight weeks post-implantation

Eight weeks after implantation, Group 2 membranes were completely biodegraded and no longer visible in subcutaneous tissue (Fig. 4B (d–f)). Group 1 membranes remained thin and visible, but were indistinct from surrounding connective tissues. Newly formed connective tissue replaced the implanted membrane and its surrounding region. Small blood vessels (Fig. 4B (c), orange arrow) and fat were observed (Fig. 4B (b, c), arrowhead). Group 3 membranes maintained a porous structure (Fig. 4B (g)), but membrane thickness decreased slightly, and the inner structure became more compact than at 4 weeks. Several inflammatory cells, blood vessels, and blood cells were observed in the areas adjacent to the surface and inside the implanted membrane (Fig. 4B (h, i), orange arrow). Group 4 membranes showed reduced thickness at 8 weeks compared to 4 weeks (Fig. 4B (j)). The membrane retained some of its porous structure, and a darkly stained, thick skeletal

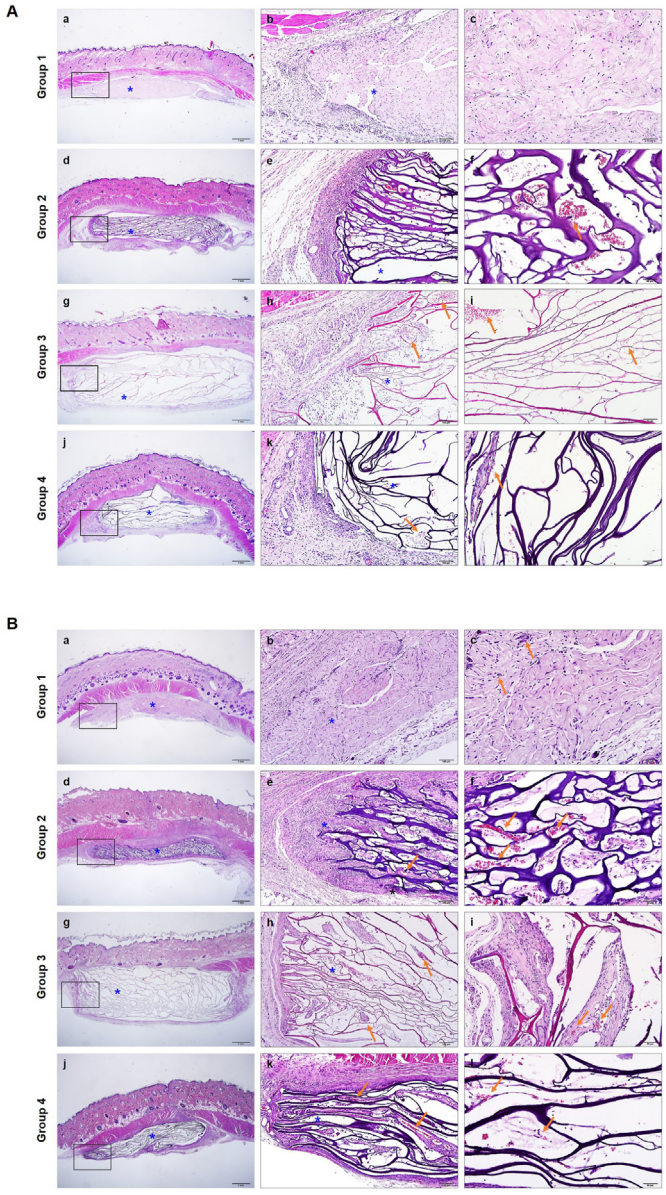

Fig. 3. Histological observation of the implanted collagen membrane after 1 and 2 weeks. Representative hematoxylin and eosin (HE) staining images of subcutaneously implanted collagen membranes. Implanted membrane region is indicated with an asterisk (*). (A) Observation of the implanted collagen membrane after 1 week. Group 1 did not maintain initial shape (square) of implanted membrane and appeared as an aggregated gel (a–c). Membranes of Groups 2 (d–f), 3 (g–i), and 4 (j–l) exhibited multilayered porous structures. Red blood cells were observed inside the membranes (orange arrows). (B) Implanted collagen membranes after 2 weeks. Numerous inflammatory cells were present in the membrane compared to that at 1 week. In particular, significant blood vessel formation was observed in Group 2 (d–f, orange arrow). First-line image scale bar: 1 mm. Middle line image scale bar: 100 μm. Last line scale bar: 50 μm.

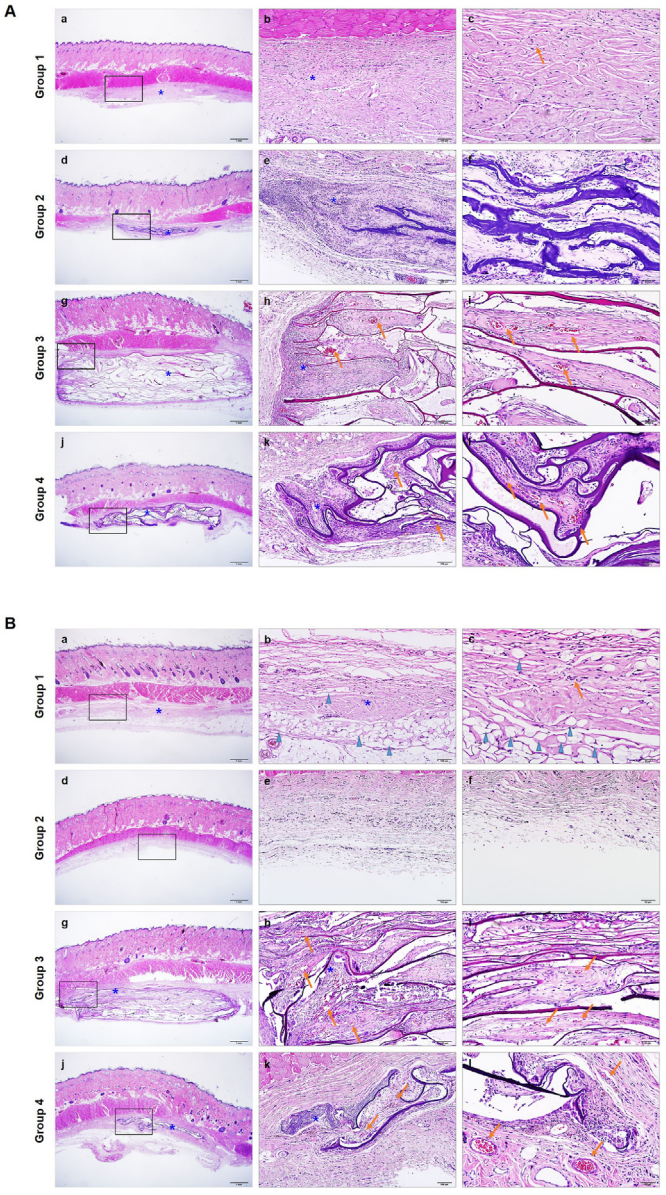

Fig. 4. Histological observation of the implanted collagen membrane at 4 and 8 weeks after implantation. Representative HE staining images of subcutaneously implanted collagen membranes. The implanted membrane region is indicated with an asterisk (*). (a) Implanted collagen membrane after 4 weeks. Numerous inflammatory cells infiltrated the membranes of all groups compared to that at 1 week. In particular, blood vessel formation was observed in Groups 3 (g–i, orange arrow) and 4 (j–l, orange arrow). (b) Implanted collagen after 8 weeks. The collagen membrane in Group 1 remained thin and visible. Small blood vessels (c, orange arrow) and fat were observed (b, c, arrowhead). The membrane had completely biodegraded in Group 2 (d–f). Group 3 maintained the porous structure of the membrane, and several inflammatory cells and blood vessels were observed inside the implanted membrane (h, i; orange arrow). The membranes in Group 4 had a porous structure and thick skeletal structure. Mature and thick blood vessels were observed inside the membrane (k, l, orange arrow). First-line image scale bar: 1 mm. Middle line image scale bar: 100 μm. Last line scale bar: 50 μm.

structure was observed. The membrane and surrounding connective tissue had no distinct boundaries. Mature blood vessels appeared inside the skeletal membrane structures, and many blood cells were observed (Fig. 4B (k, l), orange arrow).

3.8. Twelve weeks post-implantation

Twelve weeks after implantation, the overall structure of Group 1 membrane disappeared, and only a part of the membrane remained (Fig. 5a). Fat was observed in areas where the membrane had degraded (Fig. 5b, c arrowhead). The border between the surrounding tissue and the transplanted membrane was indistinguishable. Mature blood vessels were present at this location (Fig. 5c, orange arrow). In Group 2, membranes were not observed 12 weeks after transplantation (Fig. 5d–f). In contrast, the membranes of the other three groups did not undergo complete biodegradation (Fig. 5a, g, j). The membrane in Group 3 maintained

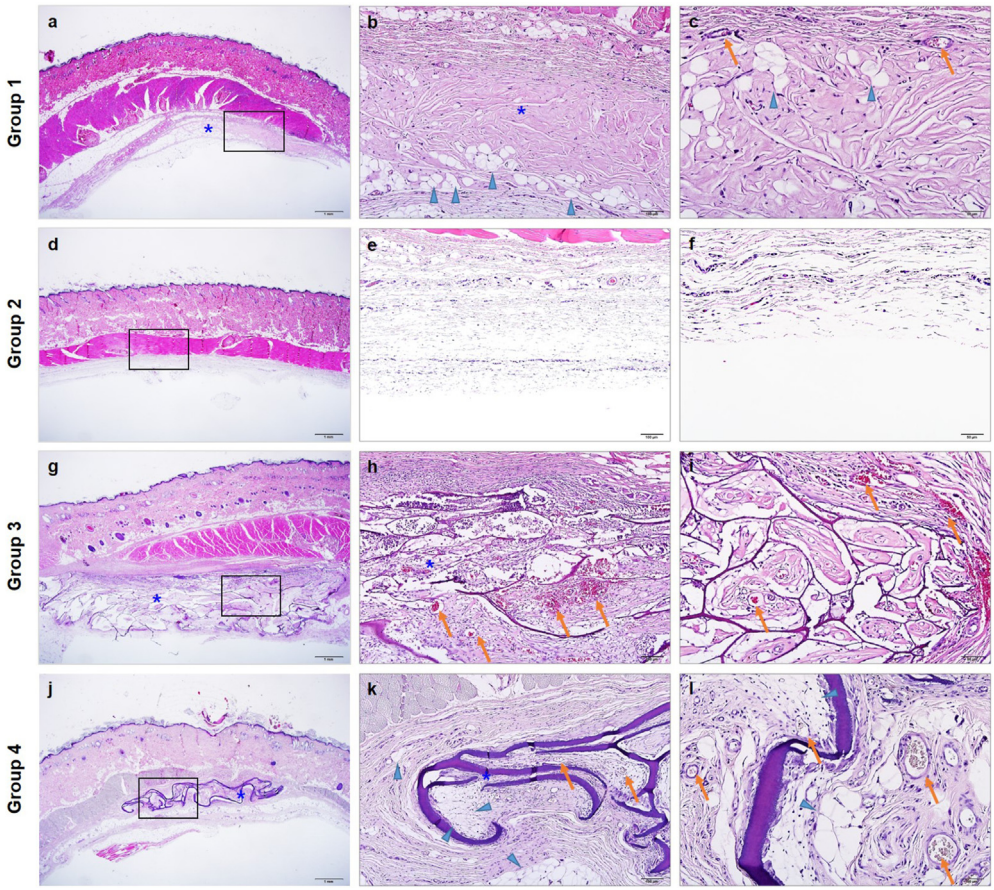

Fig. 5. Histological observation of the implanted collagen membrane at 12 weeks after implantation. Representative HE staining images of subcutaneously implanted collagen membranes. The implanted membrane region is indicated with an asterisk (*). The membrane was completely degraded in Group 2 (d–f). In Group 1, the membrane was observed only in a few parts (a–c). The membrane could be observed in Groups 3 (g–i) and 4 (j–l).

its porous structure (Fig. 5g), which remained distinguishable from the surrounding connective tissue. Many thick blood vessels were observed inside the porous structure (Fig. 5h, i, orange arrow), along with various cell types. Compared to those in the other groups, the shape, membrane thickness, and porous structure of Group 3 were better maintained. The membrane in Group 4 was still present, appearing darkly stained (Fig. 5j–l). Compared to the initial transplantation, its thickness and volume had significantly decreased. Fat (Fig. 5k, l, arrowhead) and blood vessels (Fig. 5k, l, orange arrow) were noted between the membrane's skeletal structures.

3.9. Membrane thickness

The thicknesses of the implanted collagen membranes was measured at 1, 2, 4, 8, and 12 weeks. The thickness of the remaining collagen membrane at each time point is shown in Fig. 6. In Group 1, the membrane thickness continued to decrease up to 12 weeks after implantation. Compared to that at 1 week after implantation, membrane thickness changed significantly at 4 weeks (**; $P < 0.01$), 8 weeks (***; $P < 0.001$), and 12 weeks (***; $P < 0.001$) but not at 2 weeks. The membrane thickness of Group 2 decreased significantly between 1 and 4 weeks (***; $P < 0.001$), consistent with the histological results (Fig. 4A (d-f)). The implanted membrane was degraded by 8 weeks, so histological or thickness evaluations could not be performed (Fig. 4B (d-f)). In contrast, no significant changes in membrane thickness were observed in Group 3 during the observation period ($P > 0.05$). The membrane thickness in Group 4 decreased until 8 weeks after implantation. Compared to that at 1 week after transplantation, membrane thickness decreased significantly at 2 weeks (*$P < 0.05$), 4 weeks (**$P < 0.01$), 8 weeks (***$P < 0.001$), and 12 weeks (***$P < 0.001$).

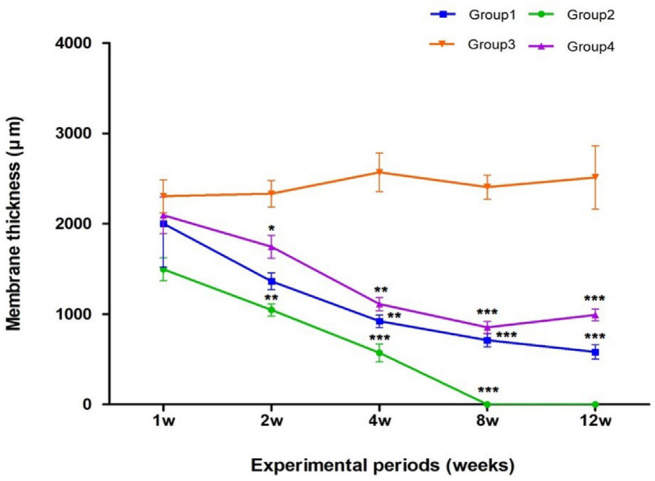

Fig. 6. Collagen membrane thickness at 1, 2, 4, 8, and 12 weeks after implantation. Membrane thickness is expressed as mean (μm) ± standard deviations derived from three samples for each implantation time point. Stars indicate statistically significant differences within groups at each time point compared with the score at 1 week (*; $P < 0.05$, **; $P < 0.01$, ***; $P < 0.001$).

3.10. Irritation evaluation of implanted membranes according to ISO 10993-6:2016

The implanted membranes were evaluated for the biological response of inflammatory cells and the overall tissue response according to ISO10993-6 standards. The response of inflammatory cell response was assessed based on the presence of polymorphonuclear cells, lymphocytes, macrophages, and necrosis. The overall tissue response was characterized by neovascularization, fibrosis, and fatty infiltration (Fig. 7a–e). The results are summarized for the entire observation period (Fig. 7f). Group 1 showed a minimum value of 2.18 at 1 week and a maximum value of 5.81 at 8 weeks, with a mean value classified as minimal or non-responsive throughout the observation period (Fig. 7f, green circle). Group 2 maintained a mean value of 8.33 at 2 weeks and 7.66 at 4 weeks, classified as a slightly irritating reaction until it disappeared via biodegradation (Fig. 7f, red square). In Group 3, the mean value increased from 4.75 at 1 week to 11.53 at 12 weeks, classified as a slight-to-moderate response. In particular, a significantly higher infiltration of inflammatory cells, such as lymphocytes and macrophages, as well as neovascularization, was observed at 8 weeks compared to Group 1 (Fig. 7f, blue triangle, $*P < 0.05$, $***P < 0.001$). Group 4 showed a mean value of 5.304 at 1 week, classified as minimal or no non-responsive, and maintained a slight response from 2 to 12 weeks. At 4 weeks, the highest value of 9.883 was observed, owing to an increase in polymorphonuclear cells, macrophages, neovascularization, and fatty infiltration, which was significant compared to Group 1 (Fig. 7f, black triangle, **; $P < 0.005$, ***; $P < 0.001$). Necrosis and fibrosis were not observed in any group.

4. Discussion

This study utilized a rat model to examine the safety (biocompatibility) and degradation (duration of membrane retention) of collagen membranes implanted subcutaneously at various time points. We analyzed inflammatory cell recruitment, fibrous tissue formation, fatty infiltration, and membrane degradation. The degradation and inflammatory responses differ between *in vitro* and *in vivo* studies, experimental sites [40,41], the selected animal model, and the membrane's origin [42]. A subcutaneous animal model is recommended for medical device evaluation according to ISO standards [43]. The rat model is widely used for biocompatibility and biodegradation studies due to its accessible implantation site, angiogenesis potential, and the membrane's protection from animal interference [44]. Additionally, it is favored for its ease of operation, standardization potential, and cost-effectiveness.

ISO 10993-6, part of the ISO 10993 series, focuses on the biological evaluation of medical devices, particularly the local effects after implantation. Small animals (e.g., rats, rabbits) are typically used, with implantation sites in muscle, subcutaneous tissue, or bone, depending on clinical application. The observation period is categorized as short-term (≤12 weeks) or long-term (>12 weeks). Evaluations include: Macroscopic Assessment (Signs of inflammation, infection, necrosis, abnormal tissue responses, and visual comparison between test and control implants); Histopathological Analysis (Tissue responses such as fibrosis, necrosis, vascularization, calcification; cellular reactions including macrophage presence, lymphocytes, foreign body reactions; tissue integration or encapsulation analysis); and Scoring System (Quantitative grading of tissue reactions).

ISO 10993-6 provides a globally recognized framework for assessing implantable medical devices, ensuring compliance with regulatory requirements (e.g., FDA, MDR) through clear test methods and criteria.

The porcine skin-derived collagen membrane used in this study primarily consisted of type I collagen. It is widely used because its 3D structure resembles a natural extracellular matrix. It has been extensively studied in animal and clinical studies for its biocompatibility and cell affinity [45,46]. Collagen source variability has been noted, with extractions from bovine and porcine tendons, skin, pericardium, and other sources [47]. Visual observation

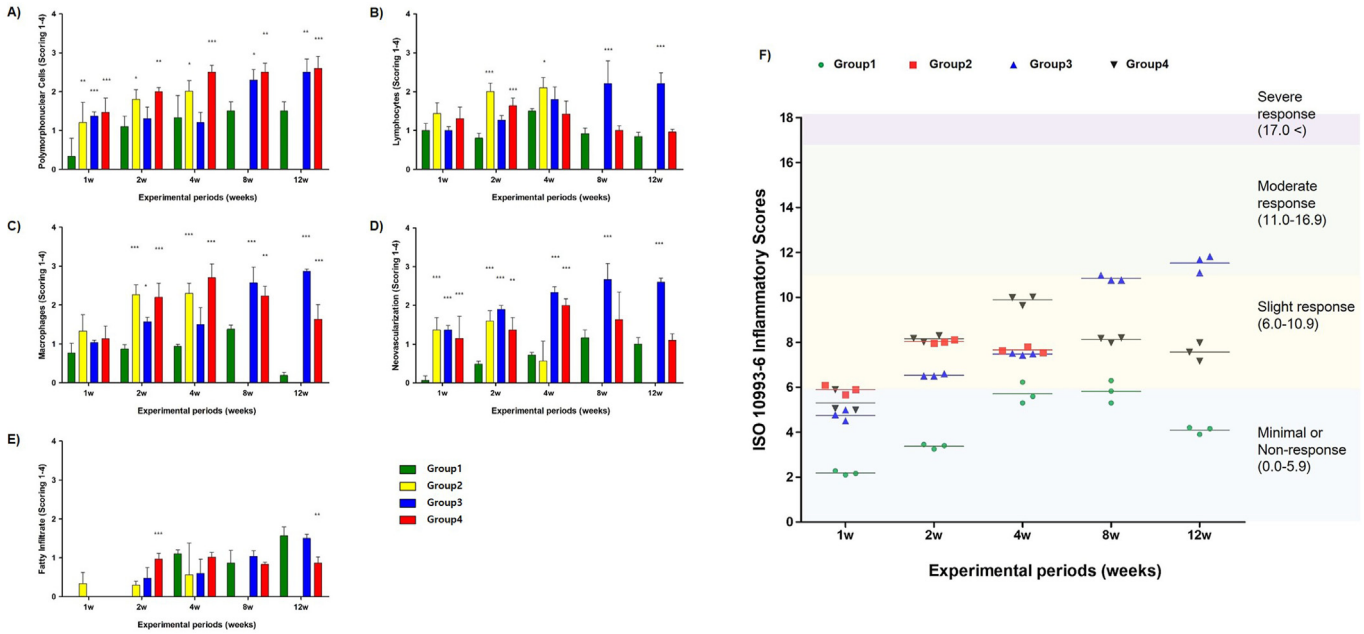

Fig. 7. Score of the inflammatory reaction induced by implanted collagen membrane. Inflammatory cell response (a–c), overall tissue reaction (d–e), and inflammatory reaction score (f) according to ISO10993-6:2016 for all groups at 1, 2, 4, 8, and 12 weeks after implantation. (a–e) Scoring results are expressed as mean ± standard deviation. Statistical analysis was performed to compare differences between groups at each time based on results of Group 1. *; $P < 0.05$, **; $P < 0.01$, ***; $P < 0.001$. (f) Results of the inflammatory reaction are presented as means. Groups were classified according to criteria ISO10993-6:2016: minimal or no-response (0.0–5.9), slight response (6.0–10.9), moderate response (11.0–16.9), and severe response (17<).

confirmed the excellent tissue compatibility of porcine skin-derived collagen membranes in experimental animals (Fig. 2).

Various cross-linking technologies have been developed to counteract the rapid biodegradation of collagen *in vivo*. The physical properties, resorption, and decomposition rates of collagen can be enhanced via chemical and physical cross-linking methods. Chemical cross-linking agents include glutaraldehyde, formaldehyde, polyepoxy compounds, acyl azide, carbodiimides, hexamethylene diisocyanate, and 1-ethyl-3 (3-dimethylaminopropyl) carbodiimide. Physical cross-linking methods include heat, DHT, UV irradiation, and C-irradiation. However, concerns persist regarding chemical cross-linking due to potential cytotoxicity from residuals or degradation products *in vitro* and *in vivo* [48,49]. In many cases, increased inflammatory response and reduced tissue integrity have been reported [49].

We produced collagen membranes using DHT and BDDE cross-linking and evaluated their long-term stability and physical properties. DHT, a common physical cross-linking method, delays biodegradation and enhances collagen-based materials without introducing additional reagents [50]. This process involves exposing collagen to high temperatures in a vacuum, removing water to form cross-links [51,52]. Key factors influencing cross-linking density and collagen properties include temperature (85–145 °C) and duration (1–7 days) [53]. BDDE, a widely used cross-linking agent in hyaluronic acid fillers, is recognized for its stability, biodegradability, and long-term safety record. Under basic conditions (pH > 7), the epoxide groups at both ends of the molecule preferentially react with the hydroxyl CH_2OH group of hyaluronic acid to form an ether bond. The stability of this ether bond ensures a long clinical duration and biodegradability [54,55]. Unreacted BDDE is not carcinogenic in mice, and there is no evidence of acute, subchronic, or chronic inflammation, according to biocompatibility tests conducted in accordance with the 1987 International Standard (ISO 10993) [56].

Histological analysis at one week showed that Group 2 membranes retained a more robust porous skeletal structure compared to Group 1 (Fig. 3). Groups 3 and 4, manufactured using BDDE, exhibited a porous structure similar to cross-linked hydrogels [57]. In contrast, the freeze-dried membrane of Group 1 became lumpy 1 week after implantation compared to the other groups (Fig. 3). Collagen membranes with different cross-linking methods and structures show differences in their biodegradation patterns, resorption times, and degrees of inflammatory cell infiltration. One week after implantation, infiltration of lymphocytes, monocytes, plasma cells, and macrophages was observed at the edge of the transplanted membrane (Fig. 3A (b,e,h,k)). Two weeks after implantation, Groups 2, 3, and 4 membranes showed a significant increase in blood cells within the porous membrane (Fig. 3B (c, f, i, l)). The porous structure of these collagen membranes facilitated cell invasion, unlike Group 1. All groups showed mononuclear cell infiltration at 4 weeks, indicating ongoing decomposition of the membrane (Fig. 4A). Collagen membrane is resorbed *in vivo* by the enzymatic activity of infiltrating macrophages and polymorphonuclear leukocytes [58]. Moreover, collagen membrane degradation can commence 4–28 days after implantation [59,60]. Particularly in Group 2, the volume of the porous membrane rapidly decreased at 4 weeks compared to Group 1 (Fig. 4A (d-f)), and it was completely degraded at 8 weeks (Fig. 4B (d-f)). Additionally, Group 4 membranes treated with BDDE and DHT lost their structural form and degraded more quickly than membranes of Group 3 treated with BDDE alone, as shown by histological observations from 4 to 12 weeks (Fig. 4A and B, Fig. 5). According to the ISO standards, these groups also showed the highest value in the membrane irritation evaluation, with an increase in PMN, macrophages, new blood vessels, and fat formation at 4 weeks (Fig. 7 (f)).

The inflammatory reaction score of Group 1 showed minimal or no response (0.0–5.9) during the 1–12-week observation period. Groups 2, 3, and 4 had higher inflammatory reaction scores than Group 1 but were evaluated within the range of a slight response (6.0–10.9), except at 12 weeks in Group 3. Furthermore, BDDE-crosslinked collagen Groups 3 and 4 did not exhibit a higher inflammatory reaction than the DHT cross-linked Group 2. These results are similar to the biocompatibility test results reported for the BDDE cross-linker [56]. Additionally, BDDE cross-linking stabilizes the structure of biomaterials, improving mechanical strength and durability [61]. In addition, the biodegradation rate [62] and physical properties of collagen and other polymers can be controlled. This was confirmed in our histological results as BDDE-crosslinked Group 3 had a slower biodegradation rate than other groups and maintained the porous structure and the thickness and shape of the collagen membrane relatively well (Fig. 4).

Many researchers have reported that DHT treatment performed on natural collagenous materials and collagen scaffolds increases their mechanical properties, due to the formation of ester and amide bonds in DHT treatment compared to non-crosslinked scaffolds [63–65]. Specifically, the strength of the scaffold increases [66]. More importantly, DHT cross-linking helps prolong the biodegradation of the scaffold [67].

However, our research results showed that groups 2 and 4, in which DHT cross-linking was performed, degraded more rapidly. As mentioned in the results, in Group 2 of lyophilized collagen, DHT degraded faster than in Group 1 of lyophilized collagen, and in Group 4 of BDDE-crosslinked collagen, DHT degraded faster than in Group 3 of BDDE-crosslinked collagen. Group 2 membrane degraded faster than Group 1, and the membrane of Group 4 degraded faster than Group 3. This is a different result from the finding that DHT cross-linking helps prolong the biodegradation of the scaffold. This may be because collagen denaturation is induced at high temperatures, which damages the triple helix structure. Consequently, the denatured part loses resistance, and its *in vivo* stability deteriorates, resulting in more rapid decomposition [68,69]. In the present study, the DHT method was used under conditions above 145 °C. Collagen denaturation is sensitive to DHT temperature and reaction duration. Denaturation can impair the mechanical properties of collagen by damaging its triple helix structure and altering the packing of collagen molecules [70]. Additionally, a higher crosslinking temperature may lead to denaturation of collagen scaffolds and natural unwinding of the triple helix. DHT treatment conducted at 145 °C or a treatment duration longer than 5 days induces severe denaturation and deterioration of mechanical properties [53,71,72]. These results show that temperature and time are critical parameters of DHT treatment used to develop collagen membranes and related products.

Environmental conditions, such as cross-linking, pH, and temperature, are used to regulate the properties and functions of collagen and are employed in various clinical trials. The type of collagen membrane (film, sheet, disc type, etc.) used in this study can also be used in various clinical applications. Collagen membranes exhibit hemostatic properties that promote blood coagulation and play an important role in tissue repair. Collagen initiates adhesion and aggregation of platelets that lead to thrombus formation [73,74]. It is also very useful in the treatment of severe burns and as a dressing for many types of wounds, such as pressure ulcers, leg ulcers, and bedsores. Collagen membrane has the ability to easily absorb large quantities of tissue exudate, smooth adherence to the wet wound bed with preservation of a low moist climate, as well as its shielding against mechanical harm and secondary bacterial infection [75]. Additionally, the absorption rate of the membrane can be adjusted through cross-linking of BDDE, making it possible to employ an appropriate dressing formulation in various wound models [76].

The rate of drug release *in vivo* can also be controlled by controlling the degradation rate through cross-linking. Collagen membranes in the form of ophthalmic implants have also been used as a drug delivery system to treat infected corneal tissue using high doses of antibiotics such as gentamicin [77] and tetracycline [78]. Biopolymer scaffolds must be tolerant of mechanical stresses for optimal reconstruction of hard tissue defects. Collagen itself was used as a bone substitute due to its osteoinductive activity [79]. In particular, the DHT cross-linked membrane used in this study is used to promote bone formation [80,81] and bone regeneration around implants and is reported to be helpful in treatment by controlling biocompatibility and degradation speed [82]. BDDE cross-linking has been used to improve the morphological and biomechanical properties of collagen bone scaffolds [83]. Cross-linked collagen is used as a scaffold to prevent adhesion after surgery and to prevent recurrence of hernias in abdominal wall defects [84]. A DHT cross-linked collagen scaffold is effective in nerve regeneration due to its improved tensile modulus [85].

Collagen cross-linking for various clinical applications may exhibit improved properties of support matrices in biotechnology. Each crosslinking method demonstrates a different degree of structural and mechanical stability, which is largely attributed to the different crosslinking mechanisms, concentration, and exposure time. To date, no gold standard protocol exists for crosslinking collagen-based materials. More suitable cross-linking methods for collagen-based materials need to be developed to achieve an appropriate balance between stability and functional remodeling in tissue engineering and regenerative medicine. We believe that our research also constitutes a helpful contribution to research on collagen-based materials.

We observed the changes in collagen membranes implanted in the dorsal region of rats for up to 12 weeks. However, one limitation of our study is that we were unable to assess long-term inflammatory responses, fibrosis, or extended degradation processes beyond this period. Therefore, based on the findings of this study, future research should extend the observation period to 16–24 weeks or longer to achieve a more comprehensive evaluation of the long-term biocompatibility and tissue response of collagen membranes. Additionally, this study was conducted using a subcutaneous implant model using rats. Application of the results of this study to specific clinical environments (e.g. bone, joint tissue, and dental) may be limited. Therefore, if application to specific clinical environments is necessary, additional research should be considered based on the results of this study.

In this study, the four groups of collagen membranes exhibited different structures and biodegradation properties. Depending on the cross-linking method, the decomposition rate and inflammatory response of the collagen membrane differ *in vivo*. The cross-linked collagen membrane exhibits a porous structure, which allows the inflow and growth of cells, enabling the creation of new tissues and cell growth. However, it can also cause rapid infiltration of cells into the membrane, which may deteriorate the membrane barrier function and cause rapid biodegradation. Therefore, the cross-linking methods involving cross-linking agents and extreme conditions, along with collagen structure, can negatively impact collagen decomposition characteristics. Therefore, these factors must be considered when manufacturing collagen membranes and developing products.

Author contributions

Go EJ, Bae BS, & Jung JW performed the experiments; Cho ML analyzed the data; Shetty AA contributed to the study's conception and background literature research; Kim SJ & Kim SA designed the study and wrote the manuscript.

Data availability

All data are available within the manuscript.

Ethics statement and patient consent

Consent was not required for this research.

Declaration of Generative AI and AI-assisted technologies in the writing process

The authors declare that they did not use AI-generated work in this manuscript.

Declaration of competing interest

None.

Acknowledgments

This research was supported by the Cultivating the Next Academic Generation Program of the National Research Foundation (NRF), funded by the Korean government (MSIT) (NRF-2022R1A6A3A01086587) and the National Research Foundation of Korea (NRF), South Korea grant funded by the Korea government (MSIT) (No. 2023R1A2C2003846).

References

[1] Sharma S, Dwivedi S, Chandra S, Srivastava A, Vijay P. Collagen: a brief analysis. Oral Maxillofac Pathol J 2019;10(1).
[2] Koláčná L, Bakešová J, Varga F, Košťáková E, Plánka L, Nečas A, et al. Biochemical and biophysical aspects of collagen nanostructure in the extracellular matrix. Physiol Res 2007;56(Suppl 1):51–60.
[3] Friess W. Collagen—biomaterial for drug delivery. Eur J Pharm Biopharm 1998;45(2):113–36.
[4] Smethurst PA, Onley DJ, Jarvis GE, O'Connor MN, Knight CG, Herr AB, et al. Structural basis for the platelet-collagen interaction: the smallest motif within collagen that recognizes and activates platelet Glycoprotein VI contains two glycine-proline-hydroxyproline triplets. J Biol Chem 2007;282(2):1296–304.
[5] Copes F, Pien N, Van Vlierberghe S, Boccafoschi F, Mantovani D. Collagen-based tissue engineering strategies for vascular medicine. Front Bioeng Biotechnol 2019;7:166.
[6] Lutolf MP, Gilbert PM, Blau HM. Designing materials to direct stem-cell fate. Nature 2009;462(7272):433–41.
[7] Kadler KE, Baldock C, Bella J, Boot-Handford RP. Collagens at a glance. J Cell Sci 2007;120(12):1955–8.
[8] Olaechea A, Mendoza-Azpur G, Valdivia E, Rasperini G. Biodegradation of three different collagen membranes: a histological study. J Osseointegration 2016;8(2):15–9.
[9] Rahmanian-Schwarz A, Held M, Knoeller T, Stachon S, Schmidt T, Schaller HE, et al. In vivo biocompatibility and biodegradation of a novel thin and mechanically stable collagen scaffold. J Biomed Mater Res, Part A 2014;102(4):1173–9.
[10] Kirrane J, Glynn L. Immunology of collagen, international review of connective tissue research, vol. 4; 1968. p. 1–31.
[11] Lynn A, Yannas I, Bonfield W. Antigenicity and immunogenicity of collagen. J Biomed Mater Res B Appl Biomater 2004;71(2):343–54.
[12] Hakuta A, Yamaguchi Y, Okawa T, Yamamoto S, Sakai Y, Aihara M. Anti-inflammatory effect of collagen tripeptide in atopic dermatitis. J Dermatol Sci 2017;88(3):357–64.
[13] Albu M, Ferdes M, Kaya D, Ghica M, Titorencu I, Popa L, et al. Collagen wound dressings with anti-inflammatory activity. Mol Cryst Liq Cryst 2012;555(1):271–9.
[14] Wang Y, Wang Z, Dong Y. Collagen-based biomaterials for tissue engineering. ACS Biomater Sci Eng 2023;9(3):1132–50.
[15] Rezvani Ghomi E, Nourbakhsh N, Akbari Kenari M, Zare M, Ramakrishna S. Collagen-based biomaterials for biomedical applications. J Biomed Mater Res B Appl Biomater 2021;109(12):1986–99.
[16] Parenteau-Bareil R, Gauvin R, Berthod F. Collagen-based biomaterials for tissue engineering applications. Materials 2010;3(3):1863–87.
[17] Zhu J, Li Z, Zou Y, Lu G, Ronca A, D'Amora U, et al. Advanced application of collagen-based biomaterials in tissue repair and restoration. J Leather Sci Eng 2022;4(1):30.

[18] Kar M, Shih Y-RV, Velez DO, Cabrales P, Varghese S. Poly (ethylene glycol) hydrogels with cell cleavable groups for autonomous cell delivery. Biomaterials 2016;77:186–97.
[19] Gu L, Mooney DJ. Biomaterials and emerging anticancer therapeutics: engineering the microenvironment. Nat Rev Cancer 2016;16(1):56–66.
[20] Kolerman R, Qahaz N, Barnea E, Mijiritsky E, Chaushu L, Tal H, et al. Allograft and collagen membrane augmentation procedures preserve the bone level around implants after immediate placement and restoration. Int J Environ Res Publ Health 2020;17(4):1133.
[21] Thoma DS, Bienz SP, Figuero E, Jung RE, Sanz-Martín I. Efficacy of lateral bone augmentation performed simultaneously with dental implant placement: a systematic review and meta-analysis. J Clin Periodontol 2019;46:257–76.
[22] No YJ, Castilho M, Ramaswamy Y, Zreiqat H. Role of biomaterials and controlled architecture on tendon/ligament repair and regeneration. Adv Mater 2020;32(18):1904511.
[23] Sawadkar P, Sibbons P, Ahmed T, Bozec L, Mudera V. Engineering of a functional tendon using collagen as a natural polymer. ACS Biomater Sci Eng 2019;5(10):5218–28.
[24] Kew S, Gwynne J, Enea D, Abu-Rub M, Pandit A, Zeugolis D, et al. Regeneration and repair of tendon and ligament tissue using collagen fibre biomaterials. Acta Biomater 2011;7(9):3237–47.
[25] Syal A, Cozzi FM, Vazquez S, Spirollari E, Naftchi AF, Das A, et al. Dural closure techniques and cerebrospinal fluid leak incidence after resection of primary intradural spinal tumors: a systematic review. Clin Spine Surg 2024;37(7):291–5.
[26] Achinger KG, Williams LN. Trends in CSF leakage associated with duraplasty in infratentorial procedures over the last 20 years: a systematic review. Crit Rev™ Biomed Eng 2023;51(2).
[27] Chattopadhyay S, Raines RT. Collagen-based biomaterials for wound healing. Biopolymers 2014;101(8):821–33.
[28] He Y, Wang J, Si Y, Wang X, Deng H, Sheng Z, et al. A novel gene recombinant collagen hemostatic sponge with excellent biocompatibility and hemostatic effect. Int J Biol Macromol 2021;178:296–305.
[29] D'Amico E, Pierfelice TV, Lepore S, Iezzi G, D'Arcangelo C, Piattelli A, et al. Hemostatic collagen sponge with high porosity promotes the proliferation and adhesion of fibroblasts and osteoblasts. Int J Mol Sci 2023;24(9):7749.
[30] Hürzeler MB, Quiñones CR, Hutmacher D, Schüpbach P. Guided bone regeneration around dental implants in the atrophic alveolar ridge using a bioresorbable barrier. An experimental study in the monkey. Clin Oral Implants Res 1997;8(4):323–31.
[31] Adamiak K, Sionkowska A. Current methods of collagen cross-linking. Int J Biol Macromol 2020;161:550–60.
[32] M. Yamauchi, G.L. Mechanic, Cross-linking of collagen, Collagen, CRC press2018, pp. 157-172.
[33] Mohammadpour M, Masoumi A, Mirghorbani M, Shahraki K, Hashemi H. Updates on corneal collagen cross-linking: indications, techniques and clinical outcomes. J Curr Ophthalmol 2017;29(4):235–47.
[34] Kondo H, Takayama T, Onizawa T, Isobe S, Tanabe N, Suzuki N, et al. Enhanced bone formation of rat mandibular bone defects with collagen membranes loaded on bone morphogenetic protein-9. J Dent Sci 2024;19(4):2114–25.
[35] Paul BF, Mellonig JT, Towle III HJ, Gray JL. Use of a collagen barrier to enhance healing in human periodontal furcation defects. Int J Periodontics Restor Dent 1992;12(2).
[36] Pitaru S, Tal H, Soldinger M, Grosskopf A, Noff M. Partial regeneration of periodontal tissues using collagen barriers: initial observations in the canine. J Periodontol 1988;59(6):380–6.
[37] Haugh MG, Murphy CM, McKiernan RC, Altenbuchner C, O'Brien FJ. Crosslinking and mechanical properties significantly influence cell attachment, proliferation, and migration within collagen glycosaminoglycan scaffolds. Tissue Eng Part A 2011;17(9–10):1201–8.
[38] Cheung DT, Perelman N, Ko EC, Nimni Me. Mechanism of crosslinking of proteins by glutaraldehyde III. Reaction with collagen in tissues. Connect Tissue Res 1985;13(2):109–15.
[39] Rothamel D, Schwarz F, Sager M, Herten M, Sculean A, Becker J. Biodegradation of differently cross-linked collagen membranes: an experimental study in the rat. Clin Oral Implants Res 2005;16(3):369–78.
[40] Patino MG, Neiders ME, Andreana S, Noble B, Cohen RE. Cellular inflammatory response to porcine collagen membranes. J Periodontal Res 2003;38(5):458–64.
[41] Luttikhuizen D, Dankers P, Harmsen M, Van Luyn M. Material dependent differences in inflammatory gene expression by giant cells during the foreign body reaction. J Biomed Mater Res B Appl Biomater 2007;83(3):879–86.
[42] Luttikhuizen DT, Harmsen MC, van Luyn MJ. Cytokine and chemokine dynamics differ between rats and mice after collagen implantation. J Regen Med Tissue Eng 2007;1(5):398–405.
[43] Gheno E, Mourão CFdAB, Mello-Machado RCd, Stellet Lourenco E, Miron RJ, Catarino KFF, et al. In vivo evaluation of the biocompatibility and biodegradation of a new denatured plasma membrane combined with liquid PRF (Alb-PRF). Platelets 2021;32(4):542–54.
[44] Luttikhuizen DT, van Amerongen MJ, de Feijter PC, Petersen AH, Harmsen MC, van Luyn MJ. The correlation between difference in foreign body reaction between implant locations and cytokine and MMP expression. Biomaterials 2006;27(34):5763–70.
[45] Bunyaratavej P, Wang HL. Collagen membranes: a review. J Periodontol 2001;72(2):215–29.
[46] Tal H. Healing of osseous defects by guided bone regeneration using ribose cross linked collagen membranes. Refu'at Ha-peh Veha-shinayim (1993) 2004;21(3):32–41. 93.
[47] Rothamel D, Schwarz F, Fienitz T, Smeets R, Dreiseidler T, Ritter L, et al. Biocompatibility and biodegradation of a native porcine pericardium membrane: results of in vitro and in vivo examinations. Int J Oral Maxillofac Implants 2012;27(1).
[48] Khor E. Methods for the treatment of collagenous tissues for bioprostheses. Biomaterials 1997;18(2):95–105.
[49] Rothamel D, Benner M, Fienitz T, Happe A, Kreppel M, Nickenig H-J, et al. Biodegradation pattern and tissue integration of native and cross-linked porcine collagen soft tissue augmentation matrices—an experimental study in the rat. Head Face Med 2014;10:1–9.
[50] Zhang Z, Ma Z, Zhang Y, Chen F, Zhou Y, An Q. Dehydrothermally crosslinked collagen/hydroxyapatite composite for enhanced in vivo bone repair. Colloids Surf B Biointerfaces 2018;163:394–401.
[51] Yannas I, Tobolsky A. Cross-linking of gelatine by dehydration. Nature 1967;215(5100):509–10.
[52] Silver F, Yannas I, Salzman E. In vitro blood compatibility of glycosaminoglycan-precipitated collagens. J Biomed Mater Res 1979;13(5):701–16.
[53] Gorham S, Light N, Diamond A, Willins M, Bailey A, Wess TJ, et al. Effect of chemical modifications on the susceptibility of collagen to proteolysis. II. Dehydrothermal crosslinking. Int J Biol Macromol 1992;14(3):129–38.
[54] La Gatta A, Schiraldi C, Papa A, D'Agostino A, Cammarota M, De Rosa A, et al. Hyaluronan scaffolds via diglycidyl ether crosslinking: toward improvements in composition and performance. Carbohydr Polym 2013;96(2):536–44.
[55] Schanté CE, Zuber G, Herlin C, Vandamme TF. Chemical modifications of hyaluronic acid for the synthesis of derivatives for a broad range of biomedical applications. Carbohydr Polym 2011;85(3):469–89.
[56] De Boulle K, Glogau R, Kono T, Nathan M, Tezel A, Roca-Martinez J-X, et al. A review of the metabolism of 1, 4-butanediol diglycidyl ether-crosslinked hyaluronic acid dermal fillers. Dermatol Surg 2013;39(12):1758–66.
[57] Zerbinati N, Sommatis S, Maccario C, Capillo MC, Grimaldi G, Alonci G, et al. Toward physicochemical and rheological characterization of different injectable hyaluronic acid dermal fillers cross-linked with polyethylene glycol diglycidyl ether. Polymers 2021;13(6):948.
[58] Tal H, Kozlovsky A, Artzi Z, Nemcovsky CE, Moses O. Long-term bio-degradation of cross-linked and non-cross-linked collagen barriers in human guided bone regeneration. Clin Oral Implants Res 2008;19(3):295–302.
[59] Owens KW, Yukna RA. Collagen membrane resorption in dogs: a comparative study. Implant Dent 2001;10(1):49–58.
[60] Zhao S, Pinholt EM, Madsen JE, Donath K. Histological evaluation of different biodegradable and non-biodegradable membranes implanted subcutaneously in rats. J Cranio-Maxillofacial Surg 2000;28(2):116–22.
[61] Wang Q, Yan H, Zhang J, Tian X, Xiao J. Engineering a durable BDDE cross-linked collagen filler for skin rejuvenation. Biomed Mater 2024;19(5):055021.
[62] Hong GW, Wan J, Chang K, Park Y, Yi KH. Decomposition and changes in in vivo post-HA filler injection: a review. J Cosmet Dermatol 2025;24(1):e16652.
[63] Gu Z, Zhang X, Yu X, Li L, Xu Y, Chen Y. Biocompatibility of genipin-fixed porcine aorta as a possible esophageal prosthesis. Mater Sci Eng C 2011;31(7):1593–601.
[64] Keogh MB, O'Brien FJ, Daly JS. Substrate stiffness and contractile behaviour modulate the functional maturation of osteoblasts on a collagen–GAG scaffold. Acta Biomater 2010;6(11):4305–13.
[65] Kamakura S, Sasaki K, Honda Y, Anada T, Matsui K, Echigo S, et al. Dehydrothermal treatment of collagen influences on bone regeneration by octacalcium phosphate (OCP) collagen composites. J Regen Med Tissue Eng 2007;1(6):450–6.
[66] Drexler JW, Powell HM. Dehydrothermal crosslinking of electrospun collagen. Tissue Eng C Methods 2011;17(1):9–17.
[67] Lie, Gao C, Mao Z, Shen J, Hu X, Han C. Thermal dehydration treatment and glutaraldehyde cross-linking to increase the biostability of collagen–chitosan porous scaffolds used as dermal equivalent. J Biomater Sci Polym Ed 2003;14(8):861–74.
[68] Pieper J, Oosterhof A, Dijkstra PJ, Veerkamp J, Van Kuppevelt T. Preparation and characterization of porous crosslinked collagenous matrices containing bioavailable chondroitin sulphate. Biomaterials 1999;20(9):847–58.
[69] Haugh MG, Jaasma MJ, O'Brien FJ. The effect of dehydrothermal treatment on the mechanical and structural properties of collagen-GAG scaffolds. J Biomed Mater Res B Appl Biomater 2009;89(2):363–9.
[70] Wess TJ, Orgel JP. Changes in collagen structure: drying, dehydrothermal treatment and relation to long term deterioration. Thermochim Acta 2000;365(1–2):119–28.
[71] Chen X, Zhou L, Xu H, Yamamoto M, Shinoda M, Kishimoto M, et al. Effect of the application of a dehydrothermal treatment on the structure and the mechanical properties of collagen film. Materials 2020;13(2):377.
[72] Weadock KS, Miller EJ, Bellincampi LD, Zawadsky JP, Dunn MG. Physical crosslinking of collagen fibers: comparison of ultraviolet irradiation and dehydrothermal treatment. J Biomed Mater Res 1995;29(11):1373–9.
[73] Liu Q, Wang C, Cheng M, Hu L, Zhang Z, Sun Q, et al. Self-Healing conductive hydrogels with dynamic dual network structure accelerate infected wound healing via photothermal antimicrobial and regulating inflammatory response. ACS Appl Mater Interfaces 2024;16(24):30776–92.

[74] Y. Cai, Q. Li, J. Wang, L. Lei, F. Zeng, Q. Liu, et al, A multi-role drug-loading hydrogel dressing for synergistic treatment of hemostasis and infected wound, Available at: SSRN 4869241.
[75] JM P. Collagen: its place in the medical device industry. Med Device Diagn Ind 1987;9:49–55.
[76] Kang HJ, Jang YJ, Park IK, Kim HJ. An evaluation of the efficacy and characterization of a cross-linked hyaluronic acid/collagen/poloxamer sheet for use in chronic wounds. J Wound Manag Res 2018;14(1):26–36.
[77] Bloomfield SE, Miyata T, Dunn MW, Bueser N, Stenzel KH, Rubin AL. Soluble gentamicin ophthalmic inserts as a drug delivery system. Arch Ophthalmol 1978;96(5):885–7.
[78] Minabe M, Takeuchi K, Tamura T, Hori T, Umemoto T. Subgingival administration of tetracycline on a collagen film. J Periodontol 1989;60 (10):552–6.
[79] Van der Heide D, Hatt LP, Della Bella E, Hangartner A, Lackington WA, Yuan H, et al. Characterization and biological evaluation of 3D printed composite ink consisting of collagen, hyaluronic acid and calcium phosphate for bone regeneration. Carbohydr Polyme Technol Appl 2024;7:100518.
[80] Ren Y, Fan L, Alkildani S, Liu L, Emmert S, Najman S, et al. Barrier membranes for guided bone regeneration (gbr): a focus on recent advances in collagen membranes. Int J Mol Sci 2022;23(23):14987.
[81] An Y-Z, Heo Y-K, Lee J-S, Jung U-W, Choi S-H. Dehydrothermally cross-linked collagen membrane with a bone graft improves bone regeneration in a rat calvarial defect model. Materials 2017;10(8):927.
[82] Lee J-H, Park S-H, Kim D-H, Jung U-W. Assessment of clinical and radiographic outcomes of guided bone regeneration with dehydrothermally cross-linked collagen membrane around peri-implant dehiscence defects: results from a 3-year randomized clinical trial. Oral Biol Res 2019;43(1):8–16.
[83] Gu L, Shan T, Ma Y-x, Tay FR, Niu L. Novel biomedical applications of cross-linked collagen. Trends Biotechnol 2019;37(5):464–91.
[84] Coccolini F, Agresta F, Bassi A, Catena F, Crovella F, Ferrara R, et al. Italian Biological Prosthesis Work-Group (IBPWG): proposal for a decisional model in using biological prosthesis. World J Emerg Surg 2012;7:1–5.
[85] Ryan AJ, Lackington WA, Hibbitts AJ, Matheson A, Alekseeva T, Stejskalova A, et al. A physicochemically optimized and neuroconductive biphasic nerve guidance conduit for peripheral nerve repair. Adv Healthcare Mater 2017;6(24):1700954.